3.3 ANALYSIS OF MOUNTAIN RIDGE ICE DETECTOR MEASUREMENTS IN UTAH DURING THE 2009-2010 WINTER SEASON

David Yorty*
Warren Weston
Mark Solak
Don Griffith, CCM
North American Weather Consultants, Sandy, Utah

1. INTRODUCTION AND BACKGROUND

Supercooled liquid water (SLW) is the target of winter cloud seeding operations aimed at snowpack enhancement in several areas of the mountainous west, including some in Utah. SLW often develops at relatively low altitudes over the windward slopes of mountain barriers during stormy weather, in many instances impinging on the higher mountain ridges, producing rime ice accumulation on trees and structures. Two new high mountain ice detector sites were established in the fall of 2009, part of an overall initiative to monitor low altitude SLW over the mountains in target areas of ongoing winter cloud seeding projects in Utah. These seeding programs utilized ground-based releases of silver iodide. An ice detector installation report was prepared and submitted by North American Weather Consultants (NAWC) in February 2010. Funding for establishment of these sites, their maintenance and data analysis has been provided by a consortium of Lower (Colorado River) Basin States (LBS) water interests as part of their support of enhancements to existing cloud seeding projects for areas that contribute to the flow of the Colorado. Funding for the LBS-funded enhancements to cloud seeding projects in Utah is administered through the Utah Division of Water Resources.

Surveys of existing meteorological stations and other prospective ice detector locations in Utah's mountains yielded a list of three priority sites, one at the Brian Head Ski Area in southern Utah, another named Skyline in central Utah above (east of) the town of Fairview, and a third near Chepeta Lake in the east-central Uinta Mountains of northern Utah. A fourth potential site at Boulder Summit in southeastern Utah has been considered as well. Their locations are shown in Figure 1. This article pertains to the Brian Head and Skyline sites that were operated for the first time within this initiative on an experimental basis during the winter of 2009-2010. Data from another ice detector site (referred to as the "Fairview" site in this article), operated for another project not far from the Skyline ice detector site, were also used in the analyses. Figure 2 shows the locations of the sites in the Skyline and Fairview areas, as well as a precipitation gage that was utilized. Additional LBS-funded ice detection sites are being established as budgets allow.

Earlier SLW measurements using ridge-top ice detectors in Utah to assess and describe winter cloud seeding potential have been reported on in Solak et al (1988) and Solak et al (2005).

Each LBS-sponsored ice detector site is located at/near the summit of a prominent mountain barrier. This has been done deliberately, so that the icing observed at each site can be considered indicative of "excess" in-cloud supercooled liquid water (SLW), i.e., SLW that is not involved in the windward slope precipitation process. This "excess" SLW can be viewed, to varying degrees depending on a few key factors, as potentially convertible via cloud seeding to precipitation reaching the surface, thus increasing the natural precipitation efficiency.

* Corresponding author address: David Yorty, North American Weather Consultants, Sandy, Utah 84093; email: dyorty@nawcinc.com

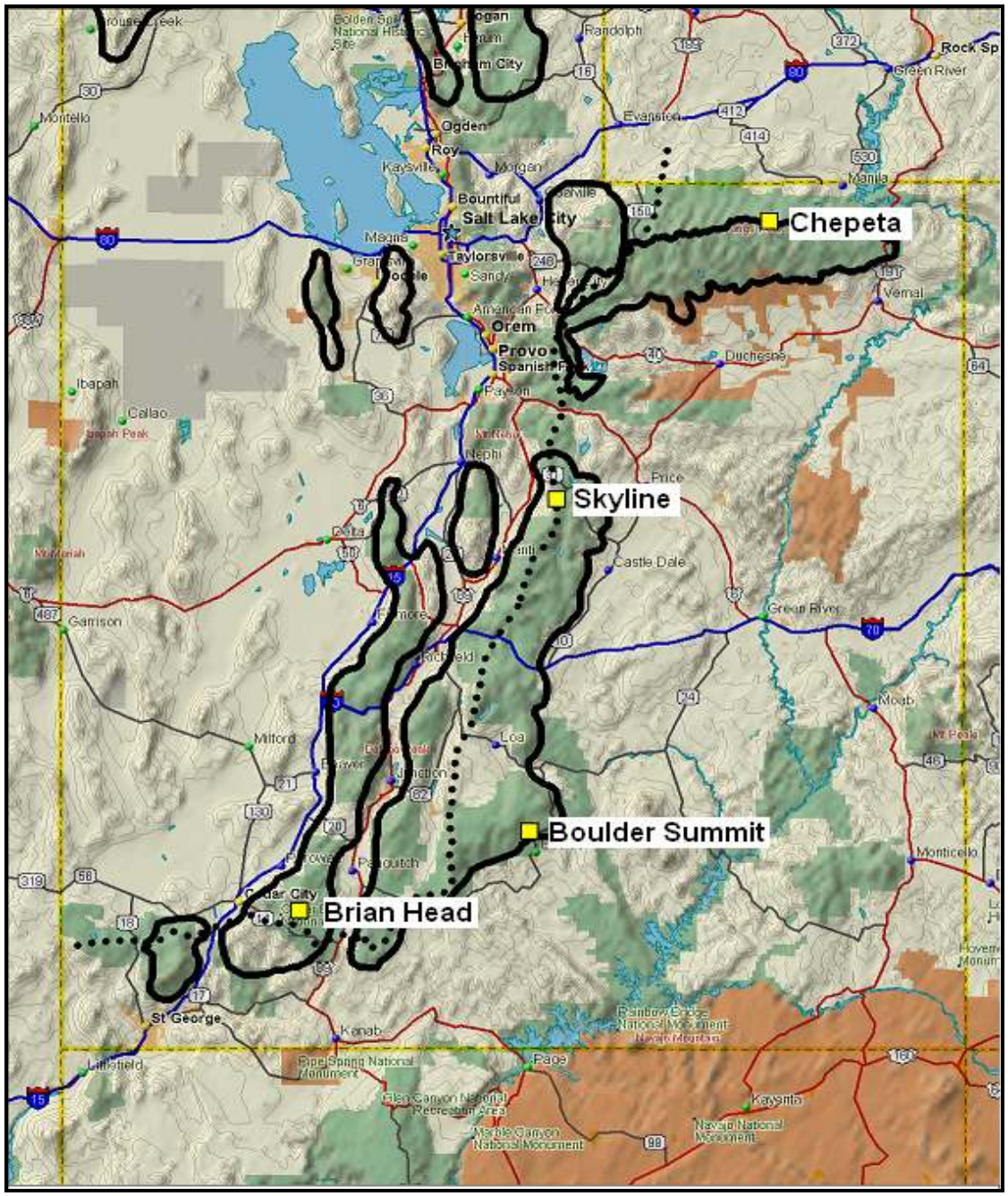

Figure 1. **Current and potential ice detector site locations (yellow squares) in Utah. The present analysis is based on sites in the Brian Head and Skyline areas. The solid lines depict operation seeding target areas, and the dotted line marks the boundary between the Great Basin (north/west) and the Colorado River Basin.**

Figure 2. Locations of ice detectors and ETI precipitation gage in the Skyline area; the distance between Skyline and Fairview sites is approximately 2.5 miles.

It should be noted that the winter of 2009-2010 was characterized as a moderate-strong El Nino situation. El Nino events are characterized by above average ocean temperatures in the eastern equatorial Pacific, and can influence weather patterns in the mid-latitudes as well. Further, the various sites' data analysis periods varied, due to their periods of operation and some instrumentation problems. The data periods available for the three ice detector sites are not complete winter seasons in all cases, but are as summarized below in Table 1.

Fairview	December 1, 2009 – March 23, 2010
Skyline	November 2, 2009 – May 31 ,2010
Brian Head	October 14 – December 8, 2009; February 17 – May 31, 2010

Table 1. Ice Detector Site Data Periods

Thus, the indications of the following analyses, although providing much useful information, should not be considered necessarily representative of long-term climatology.

2. SENSOR SUITES

The ice detecting sensor is the key measurement at each site. At each installation the Goodrich Model 0871LH1 Freezing Rain Detector is used. Its sensing probe accumulates ice during stormy conditions at temperatures colder than freezing. An internal heater deices the probe when a predetermined mass of ice is bonded to the probe via capture of supercooled liquid water droplets when the detector is in-cloud. The sensor then cools to again act as an icing sensor. A schematic of the sensor is shown in Figure 3.

The ice detector sites were also equipped with instrumentation to measure various other meteorological parameters, as described in the following sub-sections.

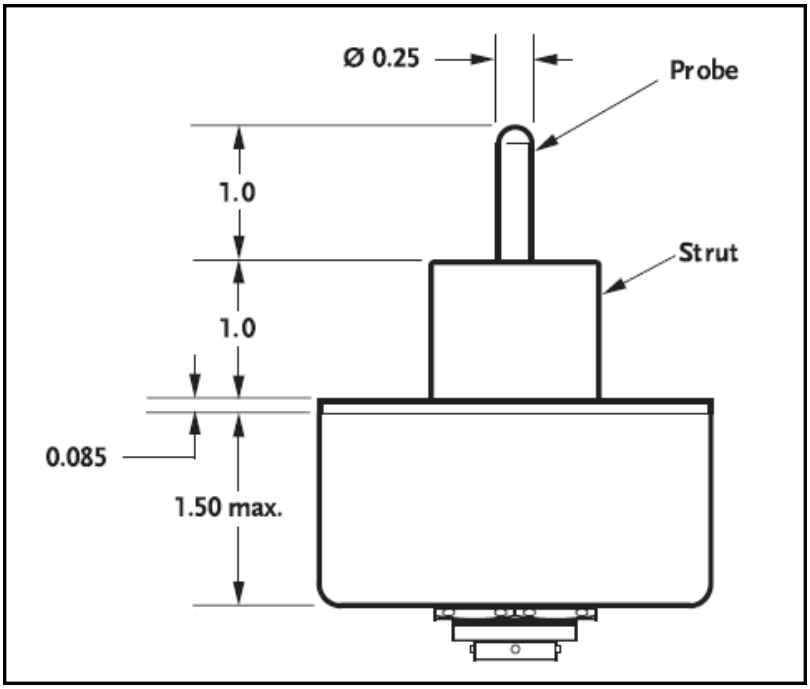

Figure 3. Schematic of Goodrich Model 0871LH1 freezing rain detector. Dimensions shown are in inches.

2.1 Brian Head

The ice detection system at the Brian Head Resort is a stand-alone installation consisting of the following.

- Goodrich Freezing Rain Detector, Model 0871LH1
- CSI Temperature Sensor, Model 107-L10
- R.M. Young Alpine Wind Speed and Direction Sensor, Model 05103-45
- Thies Precipitation Rate Sensor, Model TC041-L
- Campbell Scientific Datalogger System, Model CR1000
- Cellular Telephone Modem

Figure 4 shows the Brian Head sensor suite. The data are recorded onsite via the datalogger. Real-time data access is available via a password-protected internet link using Vista Data View software hosted by Meteorological Solutions Inc.

2.2 Skyline (Including Fairview Site)

Ice detection components have been added to an existing Utah Department of Transportation (UDOT) Skyline meteorological measurement system. The full site suite consists of the following. The components that have been added to the existing sensor suite are indicated using an asterisk.

- Goodrich Freezing Rain Detector, Model 0871LH1 *
- Temperature/Relative Humidity Sensor
- Wind Speed and Direction Sensor
- Two solar panels *
- Battery Bank for powering and deicing the ice detector*

Figure 5 shows the Skyline sensor suite. The data are recorded onsite via UDOT's datalogger. Data were available for the period of February 20 – March 19, 2010, from a high-resolution ETI weighing-type rain gage, installed and operated by NAWC in support of the project. The gage was provided by the Utah Division of Water Resources, and was installed at a location near the ice detector site.

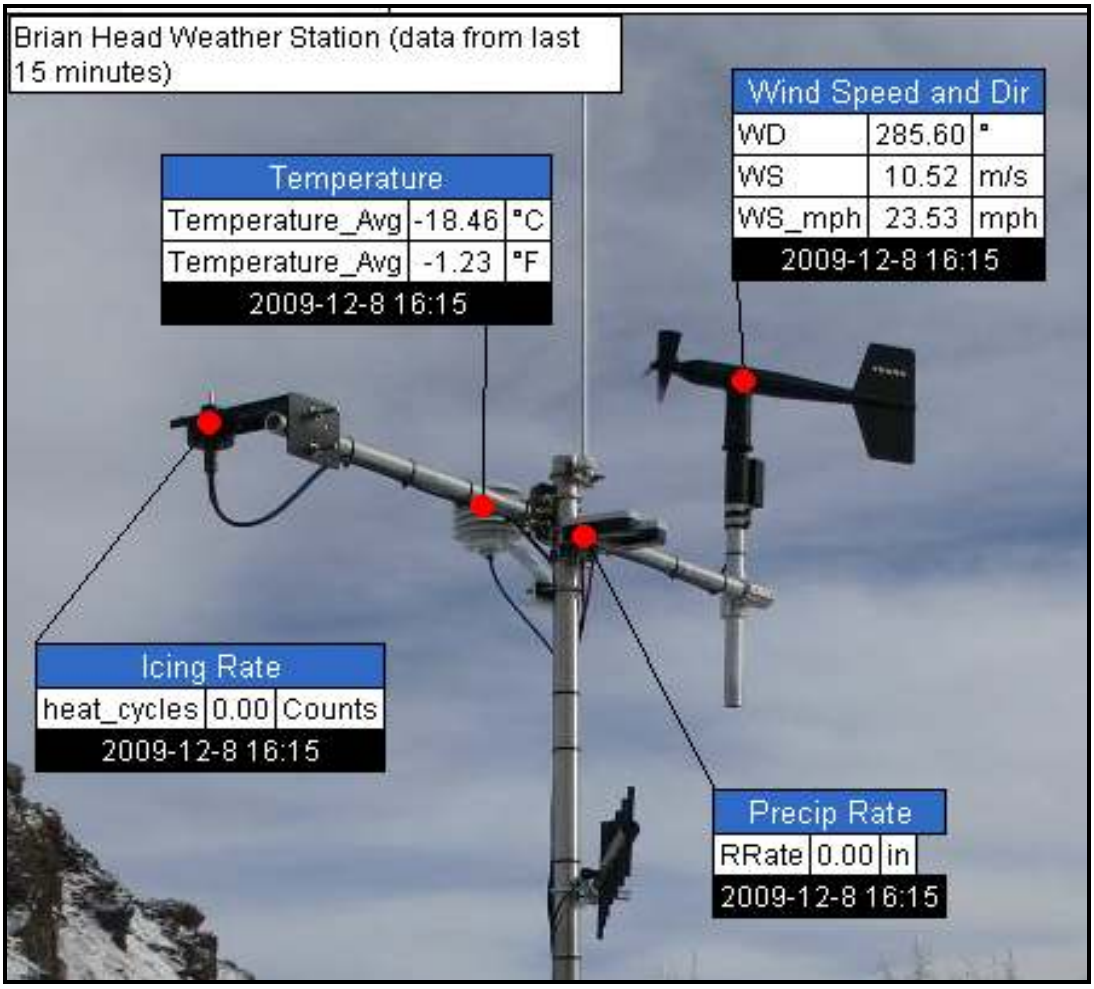

Figure 4. Sensor Suite at Brian Head

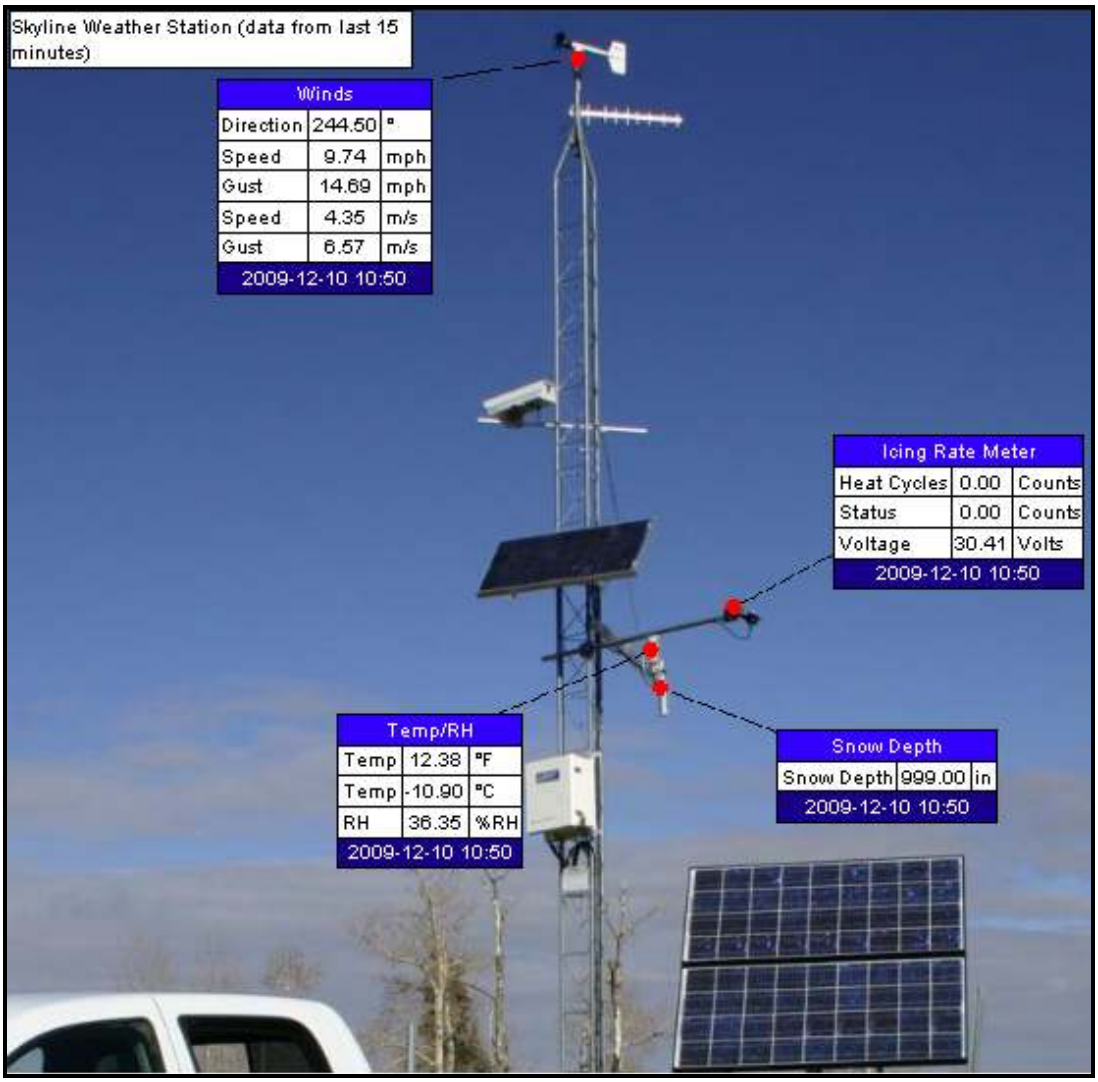

Figure 5. Sensor Suite at Skyline UDOT.

3. SEASONAL RIMING CHARACTERISTICS

Investigation of the various seasonal meteorological aspects of icing occurrences relative to other key winter storm characteristics can reveal important relationships that lead to improved seeding opportunity recognition and potentially improved cloud treatment.

3.1 Pre- vs Post-Frontal Cloud Systems

Pre- and post-frontal air masses differ by definition and their "seedability" can differ as well. The 2009-2010 winter season data have been stratified according to this distinction.

The occurrence of icing cycles at three sites (Brian Head, Skyline, and a lower-elevation site southwest of the Skyline site operated by another agency) was examined with regard to the synoptic situation for storm events during the 2009-2010 season. The observed icing was divided into five categories, based on the synoptic-scale weather situation at each measurement site when the icing was observed:

1) Pre-frontal (warm sector of storm event, no cold frontal passage observed yet at the site).
2) After cold front and before main trough axis ("katafront" situation).
3) Behind the main trough axis.
4) Associated with a closed low.

5) Associated with a zonal (westerly flow) pattern, or difficult to define the synoptic situation based on available data.

All of the first three synoptic situations are believed to be well represented in the data, and generally are of a similar time duration. Results of the analysis are shown in Figures 6a – 6c, for the two newly installed LBS-funded sites (Brian Head and Skyline), plus the cooperator site called Fairview. Icing at all three sites was more frequent during post-trough situations than for the other synoptic categories. This post-trough icing represented approximately 50% of the icing events at Brian Head, 51% at Skyline and 39% at the lower Fairview site. The second category (between cold frontal passage and main trough axis) represented the next most frequent icing at two sites (Brian Head and Skyline). The lower Fairview site had more frequent icing in the "pre-frontal" and "zonal or undefined" categories than in the #2 category, although a much shorter observational season at that site leads to the data being highly influenced by specific storm events (in particular, one on December 12-13) and probably less representative as a whole. Pre-frontal icing accounted for 14% at Brian Head and 9% at Skyline, with the 22% in this category at the lower Fairview site, almost of which occurred during an extremely active storm event on December 12-13, 2009.

The "zonal or undefined" category represented about 6-10% of the icing at Brian Head and Skyline (similar to the overall share in the "closed low" category) and a larger percentage (19%) at the lower Fairview site. Icing associated with "closed low" types of systems was fairly minor, representing between 4-7% of total icing at the sites. When the three sites' indications are combined by averaging the percentages within the five synoptic stratifications (Figure 7), the post-trough icing represented 47% of the observed icing; icing following the cold front, but before trough axis passage, was next at 21%; pre-frontal icing was third at 15%; zonal or otherwise undefined situations represented 12% of the icing; and closed-low situations represented 6% of the total icing observed.

There was some ambiguity in classification of the synoptic systems, particularly those which developed into closed-low types as they moved into the Four Corners region. A good example of this is a system on March 12-14, 2010. Originally the post-trough icing during this event was put into the "closed low" category since the system became a closed low during that time period. However, the post-trough category is probably more appropriate given the well-defined trough passage over southern Utah, as well as the classification of significant pre-frontal icing associated with this same system. The closed low category is best reserved for systems that have a well-defined closed circulation during most of their time of impact, making it difficult to identify relevant cold front or trough passage times.

These analysis results are particularly valuable in highlighting when seeding opportunity occurs during storm sequences in southern and central Utah, helping to sharpen our operational procedures and convincing us of the real-time and post hoc value of the ice detector measurements.

3.2 Riming/Precipitation Relationships

The relationship of icing (riming) occurrence to area precipitation was investigated, via comparison of icing to time series of precipitation occurrence at the Brian Head site (due to the availability of the high-resolution optical precipitation sensor). A question arose in this comparison regarding the appropriate precipitation threshold, since the highly sensitive precipitation sensor often records extremely light precipitation values during times that are probably more realistically considered non-precipitating periods when scaled against periods of significant precipitation. These light values could be due to small ice crystals associated with nucleation in the supercooled cloud, or due to blowing snow, etc. The precipitation minimum threshold chosen for the analysis was 0.01 in/hr (0.025 cm/hr), which is equivalent to about 0.1 in/hr (0.25 cm/hr) of snowfall. Figure 8 shows the results of this analysis. Nearly half (~45%) of the icing was observed to occur between precipitation periods within a storm event. About a quarter (26%) was observed during precipitation periods, with about 19% after storm precipitation had ended and about 8% of the icing observed before storm precipitation began. The analysis also indicated that approximately 3% of the icing events were associated with storm events that produced no precipitation reaching the minimum threshold.

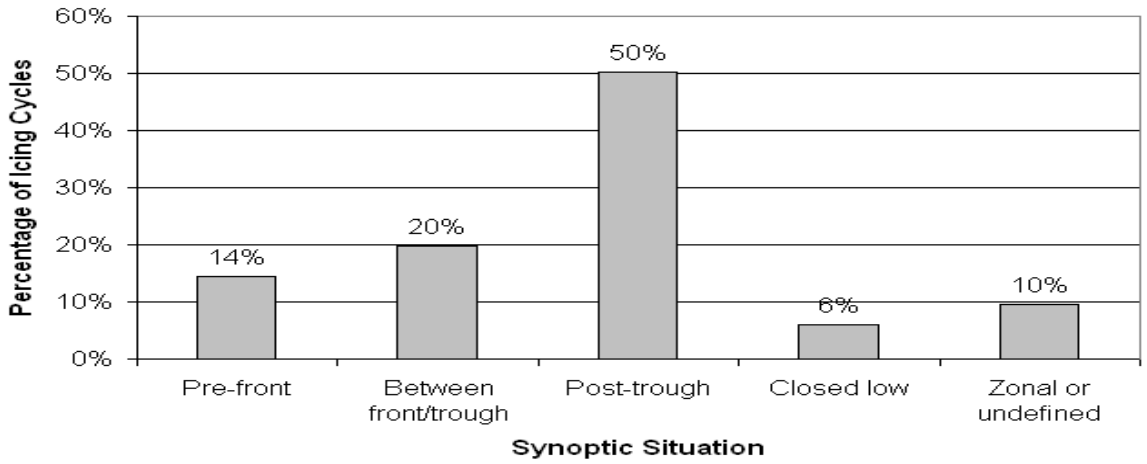

Figure 6a. Synoptic Pattern During Icing Periods, Brian Head

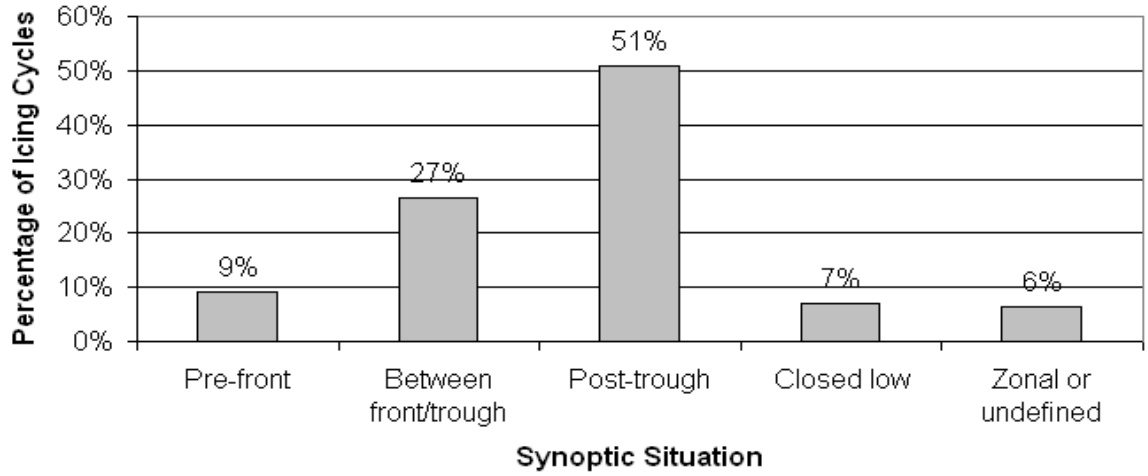

Figure 6b. Synoptic Pattern During Icing Periods, Skyline

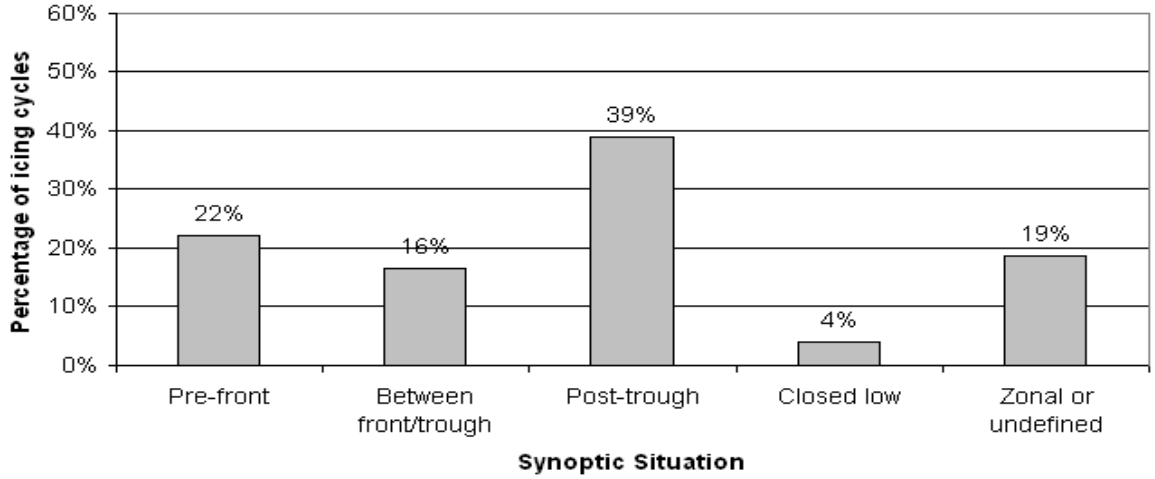

Figure 6c. Synoptic Pattern During Icing Periods, Fairview

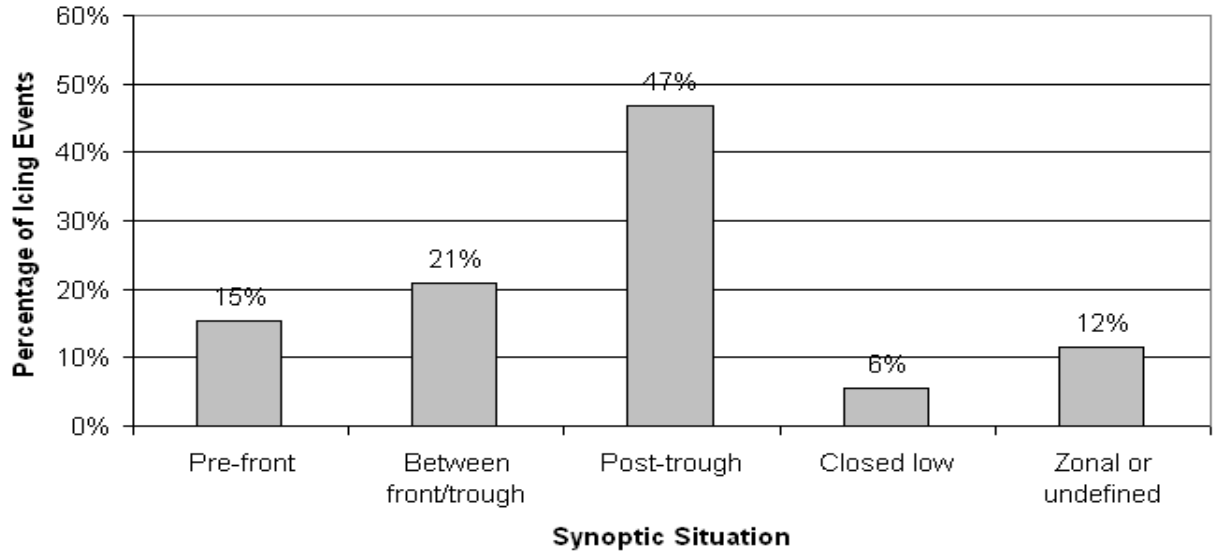

Figure 7. Synoptic pattern classification during icing periods, three-site average, 2009-2010.

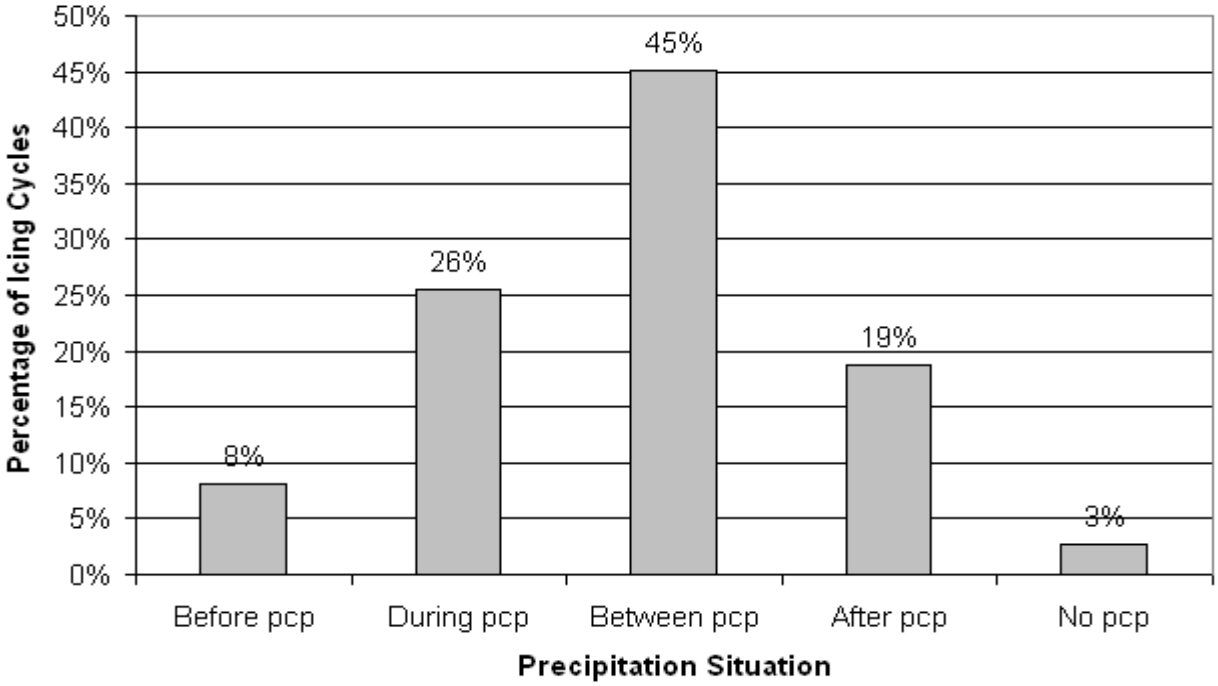

Figure 8. Brian Head Icing Distribution with Respect to Precipitation Periods During Storm events, 2009-2010.

The available Brian Head data also suggest that icing which begins prior to the initial onset of storm precipitation usually begins within a few hours of the onset of precipitation, while icing may be more likely to continue for several hours, and occasionally 12+ hours, after storm precipitation ends.

These results are quite valuable. The results point out that seeding opportunities can persist for a few to several hours after precipitation has ended in a given storm sequence. This has been suspected in the past, but these data provide confirmation and a better sense of the duration and magnitude of the seeding opportunity. The late stages of a storm are frequently characterized by colder air masses, which is important for seeding given the greater effectiveness of silver iodide at colder temperatures. Also, post-trough situations tend to be associated with a greater occurrence of lower- and mid-level moisture, in contrast to pre-frontal situations when upper-level moisture is often predominant in Utah's climate. Thus, these post-trough and post-precipitation periods can present very good seeding opportunities, especially if the air mass has become well mixed in the layer between the valley floor and mountain crest height.

3.3 Storm Period Temperature Structure

The temperature structure of the cloud bearing layer below about 500 millibars (mb), which is about 18,000 feet (~5500 m) in elevation, is a major factor regarding the seedability of a given cloud system. Three key factors pertaining to the atmospheric temperature structure, especially in relation to use of ground-based seeding, are:

- The height of the seeding material maximum (warm) nucleation activation temperature threshold (~ -5°C) relative to the mountain barrier height
- The absolute temperature range within the SLW layer, since that affects natural and induced ice particle habits (shapes) and their growth rates
- The degree to which the atmosphere from the surface to the top of the SLW layer is stable or unstable.

The temperature factors can be reasonably well assessed (accounted for) by monitoring of the mountain barrier summit temperature, and the stability issue is more fully explored in the next sub-section.

The maximum (warmest) nucleation activation temperature threshold for the fast-acting silver iodide formulations acting as condensation-freezing nuclei, as used in Utah, is about -4°C to -5°C, with the nucleation rate increasing exponentially as the temperature drops below this threshold. For ground-based seeding releases in (especially) stratiform clouds, it is thus thought that cloud systems with mountain summit temperatures warmer than about -4° offer little opportunity for enhancement. This is due to the relatively weak upward vertical air motion associated with the more-stratiform cloud types. Orographic (terrain-induced) lift can help loft ground-based releases, but close consideration must be given to the prevailing wind velocities at varying heights and the barrier shape in terms of the time (distance) available for ice particle growth and eventual fallout into the intended target region. Research has shown that seeding plumes from ground-based releases fairly commonly rise to 1,000 feet (~300 m) or more above the terrain, even in stratiform situations. Convective cloud types can loft the seeding material higher into the SLW zone, allowing effective ground-based treatment in somewhat warmer situations. Airborne seeding could potentially be more effective in warmer/stratiform circumstances if other conditions (e.g., winds and SLW concentrations) are favorable. Ground-based seeding with liquid CO_2 or propane can expand the warm end of the seedable temperature range somewhat if certain cloud conditions and barrier configuration factors are satisfied.

Earlier research has indicated that the natural precipitation efficiency of some cloud systems can be quite high and that glaciogenic seeding of those cloud systems will likely not yield appreciably more precipitation than is occurring naturally. Naturally high production of ice particles in these clouds is thought to produce near-optimum ice particle concentrations in the precipitation formation regions of the clouds. It is generally thought that this condition exists if the mountain-top temperature is colder than approximately –15° to –16° C.

The data from the three ice detection sites were analyzed to characterize the seasonal temperature characteristics from the cloud seeding

perspective. The ice detector site at Brian Head is at 10,900 feet (3350 m) elevation, at or above the summit height of the mountainous terrain in the region, with the only exception being nearby Brian Head Peak at 11,300 feet (3475 m). The Skyline site is at the summit of the mountain ridge at 9,330 feet (2870 m). The cooperator site named Fairview is located ~ 2 miles southwest of the Skyline site at about 8,700 feet (2675 m) elevation. Figure 9a shows the seasonal distribution of barrier height temperatures at the Brian Head site during each 15-minute period with sufficient icing to trigger the detectors' de-icing heater. The more southerly location of Brian Head is thought to make it more prone to warmer summit temperatures. However, as seen in Figure 9, a large proportion (~86%) of the icing periods there occurred within the favorable summit temperature window of –4°C to –16°C. This is an important and encouraging finding. Approximately 13% of the icing periods were warmer than –4° C, and <1% were colder than –16° C. Similar plots for the Skyline and Fairview sites are shown in Figures 9b and 9c, and combined results for the three sites are shown in Figure 10.

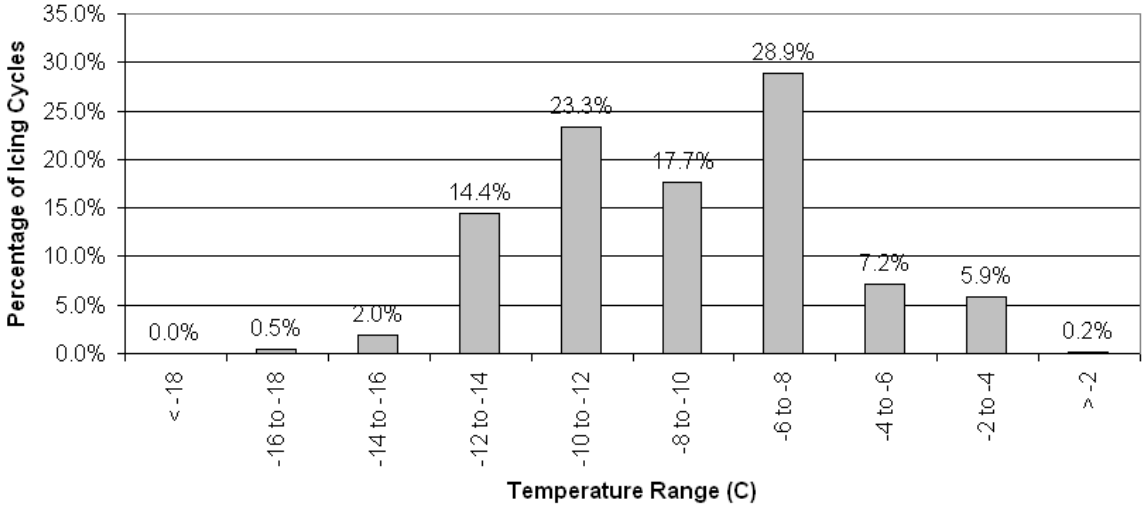

Figure 9a. Temperature Distribution During Icing Periods at Brian Head.

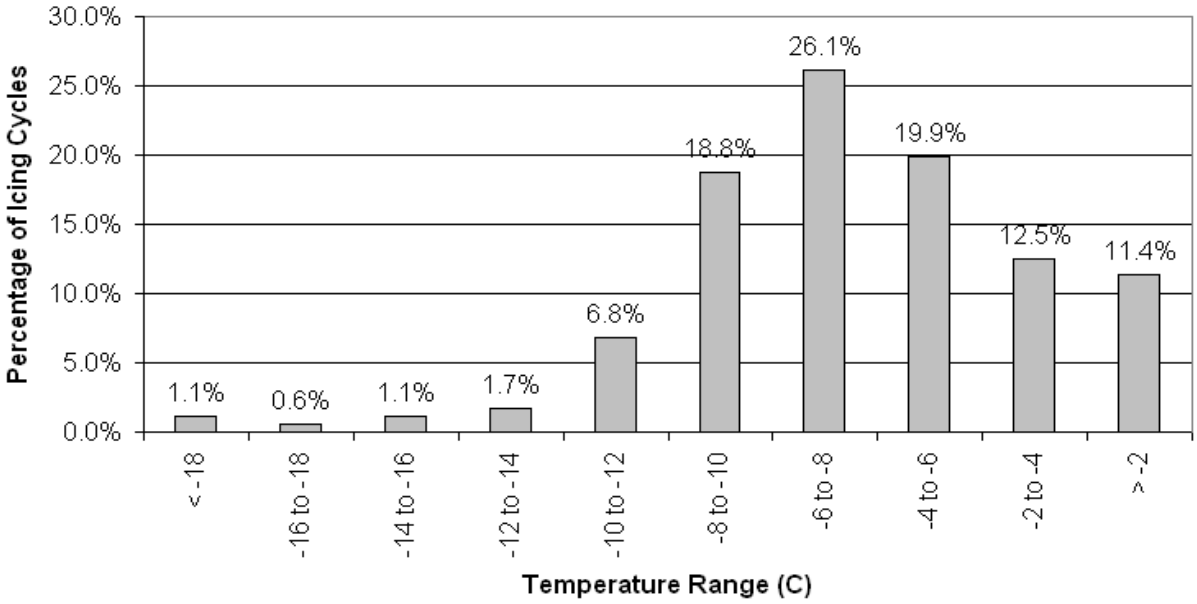

Figure 9b. Temperature Distribution During Icing Periods at Skyline.

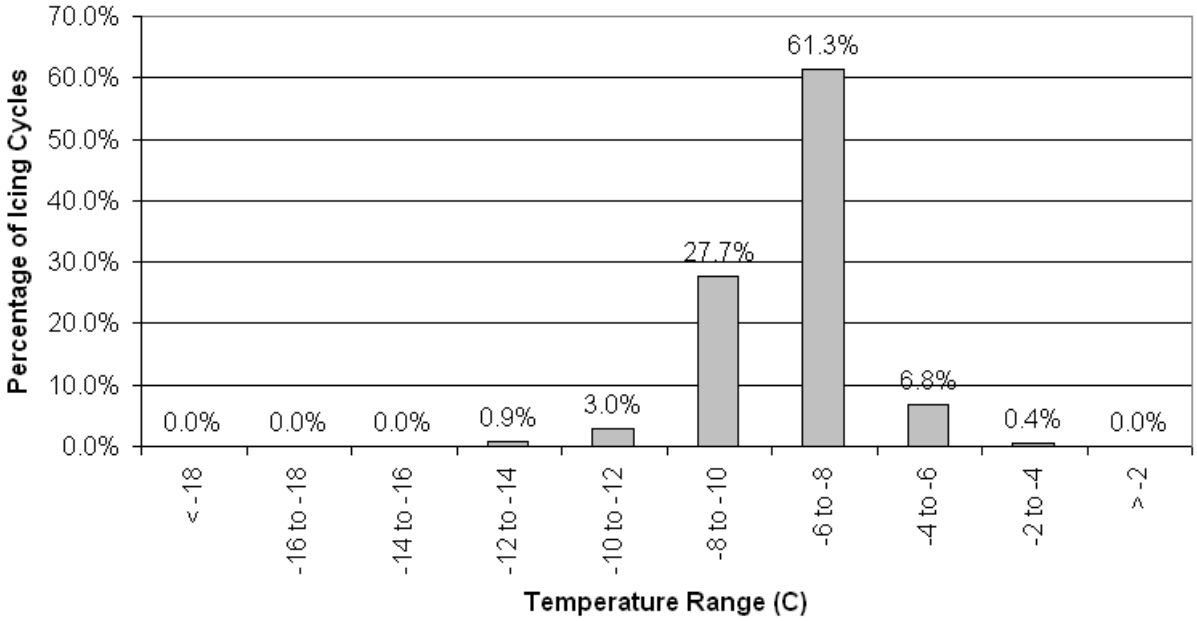

Figure 9c. Temperature Distribution During Icing Periods at Fairview.

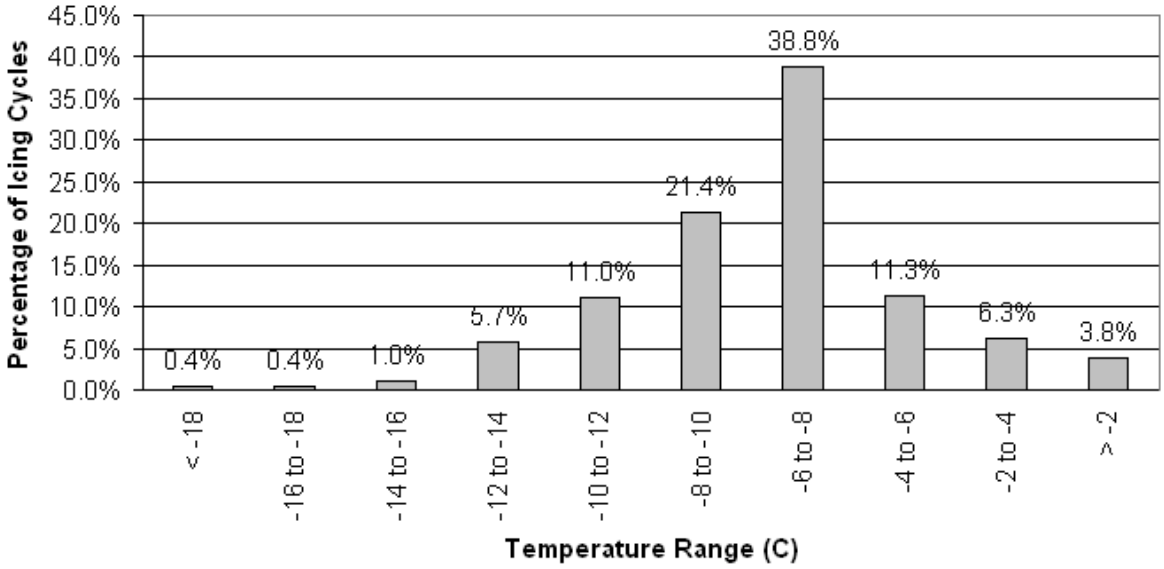

Figure 10. Temperature Distribution During Icing Periods, 3-Site Average.

3.4 Atmospheric Stability

To affect precipitation increase by cloud seeding, silver iodide particles must reach supercooled cloud regions at $\leq$-5°C to nucleate SLW droplets. Over mountainous terrain during the winter months in Utah, SLW has been shown to frequently develop at low altitudes (< 1 km) above the terrain on the windward slopes. This is the pool of SLW to be tapped by cloud seeding. If the stormy air mass has a stable temperature lapse rate, valley level silver iodide releases can be trapped, i.e, their upward vertical transport inhibited. Conversely, in an air mass exhibiting an unstable lapse rate, seeding plumes are readily lofted by thermals and orographic lift. Thus, it is important to assess the icing data with this factor in mind.

NAWC utilized data from surface sites (accessed via Mesowest) to estimate low-level thermodynamic stability during storm events related to the 2009-2010 ice detector data set. This stability is sometimes referred to as a temperature inversion, although a true inversion (where temperature increases with height in a given layer) is really only a subset of possible stable temperature profiles. Temperature and dewpoint information at Spring City (5,800 ft or 1785 m) south-southwest of the Fairview area, was compared to site temperatures at Skyline (9,330 ft or 2780 m) during icing periods. Some surface observations at Cedar City (5,600 ft or 1720 m) were compared to the site temperature at Brian Head (10,900 ft or 3350 m) during major storm periods that involved icing. A more comprehensive analysis was done for the Skyline site, since its mountain-valley upwind terrain renders that region more prone to development of low level temperature inversions and stable layers. Referencing a skew-T plot allowed the dry and moist adiabatic lapse rates to be compared to the observed differences in temperature between a corresponding valley and mountain site during storm periods with icing, with the dew point from the valley site used to determine the appropriate lapse rate(s) to use for comparison. This allows an estimate of whether or not the atmosphere is freely mixing from the surface to the elevation of the downwind mountain barrier summit, and in cases where there is stability, an estimate of the overall degree of stability in this layer. This thermodynamic stability is expressed here in terms of the temperature increase at a valley location, or decrease at the crest height, that would be needed to overcome the stability and allow free vertical mixing in the layer.

Thermodynamic stability was divided into four categories, shown in Table 2 below.

Stability Classification	Description
0	Well-mixed, with no apparent stability in the layer
1	Slightly stable (≤ 2°C surface heating to overcome stability)
2	Moderately stable (2-4°C surface heating to overcome stability)
3	Very stable (>4°C surface heating to overcome stability)

Table 2. Stability Classifications

A well-mixed situation implies that there is no thermodynamic restriction of upward vertical atmospheric motion that would impede the lifting of seeding material from a valley or foothills seeding site. A slightly stable situation would likely be seeded also, as there is a chance that forcing due to existing wind fields may be enough to overcome such a minor amount of stability, or that local temperature variations of a few degrees could easily result in areas of good vertical mixing. Seeding from valley sites would generally be avoided in a moderately or very stable situation, although seeding material initially trapped by a thermodynamically stable atmosphere may sometimes become effective later if the situation changes.

For the Skyline site, it was found that during the period November – April when the site temperature (at approximately the 700-mb level) was between –5° and –15°C, about 79% of the icing periods were associated with a generally well-mixed atmosphere down to the valley floor. Another roughly 12% of these periods were rated as "slightly stable", for a total of 91% where seeding would likely be effective. It was also noted that there was very little stability observed during the spring months beginning about March 1, so that the late-season extension period for the Lower Basin States (which normally begins mid-March) would likely be generally free of any seeding limitations due to low-level stability. The seasonal distribution of stability for the Skyline area is shown in Figure 11.

In the Brian Head area during the 2009-2010 winter season, stability during storm/icing events was found to be infrequent. Only a few cases of

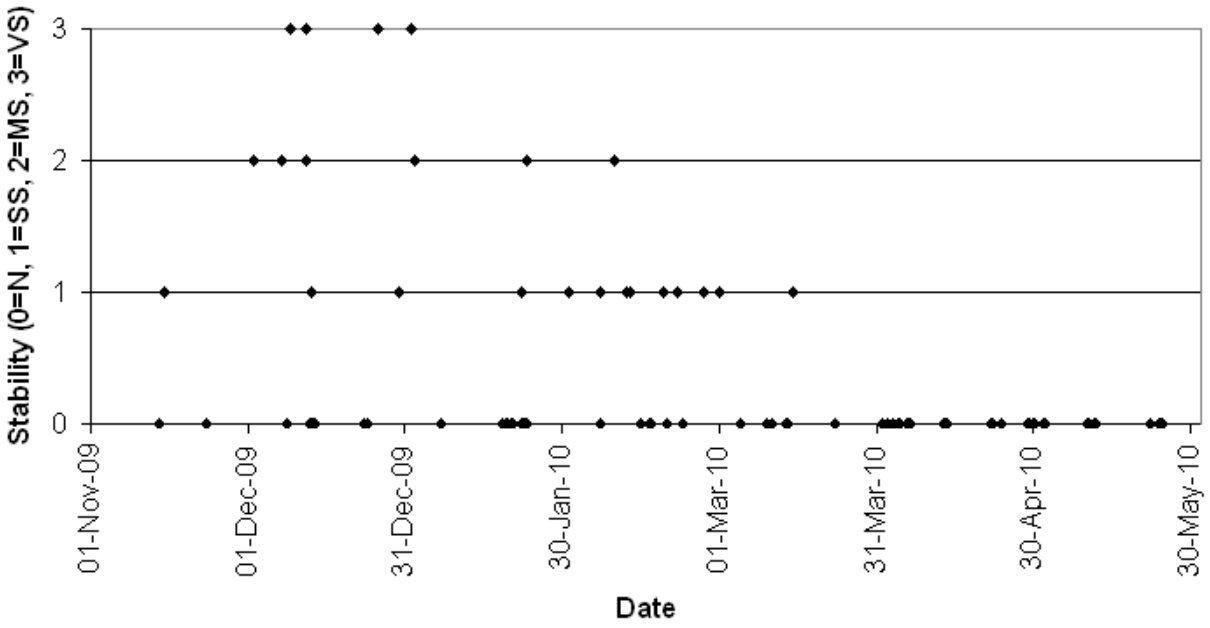

Figure 11. Seasonal distribution of atmospheric stability categories during icing periods at the Skyline detector site.

low-level stability were noted, sometimes occurring only briefly during a cold frontal passage. Late-season storm events (March – May) were nearly all associated with a well-mixed atmospheric profile.

These findings are significant in that they focus on stormy periods when SLW is being generated by orographic lift. The focus on periods with seeding potential provides a much more meaningful assessment of seasonal seedability and determination of the appropriate treatment strategy. Stated in other terms, it addresses head-on the question of the potential for ground-based seeding material releases from valley and foothill locations to effectively capitalize on seasonal seeding opportunities.

4.0 CASE STUDY: BRIAN HEAD, MARCH 12-14, 2010

Analysis of individual storm periods can also reveal useful information regarding the characteristics of the storm types that present significant seeding opportunity, including the synoptic weather patterns most likely to produce good seeding candidates in Utah. Further, seedability can vary considerably within storm periods. The case study approach sheds useful light on the factors that are important to seedability as storm systems evolve and traverse Utah.

Glaciogenic cloud seeding aims to increase the efficiency of clouds in precipitation production. One way to conceptually characterize the apparent seedability of a given cloud regime is to compare the amount of "excess" SLW measured at the mountain-top ice detection sites to the area precipitation being produced by the cloud system. In Utah, time-resolved records of these two basic parameters have been used to explore the evolution of this relationship. For example, Solak et al (2005) showed some demonstrative examples using similar data obtained in the mountains east of Salt Lake City. Stormy periods with relatively high riming (icing) and low precipitation rates exhibited low relative precipitation efficiency. Other periods showed the opposite, indicating comparatively high relative precipitation efficiency. In some cases, distinct and orderly shifts in efficiency were shown to coincide with changes in identifiable cloud characteristics.

This section summarizes one of the more demonstrative storm periods for the Brian Head site, which occurred on March 12-14, 2010. For simplicity, as well as consistency with the time labels in the graphs, all time references in the case studies are in Mountain Standard Time (MST).

4.1 Case Study Summary

A storm system moved onshore in the western U.S. on March 12-13. The core of the system moved onshore near Oregon, then southeastward into the Great Basin on the 13th and to near the Four Corners area by early on March 14. An associated cold front moved into Utah beginning during the morning of March 13. The entire system became more compact in size as it crossed the region, and also developed a closed circulation by the time it reached the Four Corners region by early on the 14th. The pre-frontal 700-mb wind pattern was southwesterly over Utah early on the 13th, with a 700-mb temperature near –3 C over most of the state. By 00Z March 14 (1600 MST on the 13th), the 700-mb temperature had dropped to near or below –10°C in portions of western and southwesterly Utah, with winds shifting to northwesterly. Winds had shifted to northerly by early on the 14th, with the 700-mb temperature near –7° to –8°C over most of Utah, as the system was developing a fairly strong closed circulation pattern.

Data from the Brian Head site clearly shows a cold frontal passage beginning just before 1400 MST on the afternoon of March 13, with the temperature dropping sharply from near –7° to around –12°C within a couple of hours. The site temperature dropped to a minimum of around –14° on the evening of the 13th, before slowly warming, rising to near –10° or above during the day on the 14th. Site winds exhibited a sharp shift from near 200 degrees (SSW) to > 300 degrees (NW) with the frontal passage, then gradually shifted to N and then NNE overnight and into the day on the 14th. Wind speeds averaged about 20-25 mph pre-frontally and with the front on the 13th, then peaked near 40-45 mph from the north around midnight (13th – 14th) and returned to the 20-30 mph range on the 14th.

This was a case where strong icing occurred both pre-frontally and post-frontally. Icing began around 0700 MST on the 13th and steadily

increased to 4+ cycles/hour by midday. A time series of precipitation, temperature and ice detector cycles is shown in Figure 12. The temperature during this pre-fontal icing period was between –7° to –8° at the site. A band of moderate – heavy precipitation lasting about 1.5 hours accompanied the front during the afternoon, and was also accompanied by a rapid end to the recorded icing activity. Another period of significant precipitation occurred in the evening from about 1730 to 2000 MST, with a few hours of lighter precipitation in between these two periods. Some light to very light precipitation was then measured into the early morning hours of the 14th. Icing activity was absent during most of the more significant precipitation periods, not resuming until around 2100 MST on the 13th. There were a couple of icing cycles around 2100 accompanied by at least some showery precipitation activity through about 2300. Icing activity then increased during the early through mid-morning hours of the 14th, with the site temperature generally in the –12° to –14° C range during most of this time with N-NNE winds. Icing ended before about 1000 MST on the 14th, with the exception of one icing cycle recorded later in the day (around 1900 MST).

Satellite images show a thickening mid-level cloud deck over the area during the morning to midday hours on the 13th, associated with the first peak in icing activity. Cloud texture in visible images through that time period suggests limited vertical development, with IR images also showing colder tops to the north and west in association with the primary frontal band. Radar imagery shows precipitation beginning around 1300 MST (still pre-frontal) just as the icing activity drops off (see Figure 13, about an hour prior to this). A visible satellite image at 1400 MST shows a thick cloud band over the area in association with the frontal passage (Figure 14), with the cloud texture in this image indicative of deeper development. Much colder tops accompany the primary frontal/precipitation band through the afternoon (see IR satellite image in Figure 15), and radar imagery shows a least moderate reflectivity (25-35 dbz) with development upward to around 25,000 feet (7700 m) in the VAD wind profile with the frontal band passage. A radar image during this time period shows the main frontal precipitation band (Figure 16). Relatively cold cloud tops and associated precipitation continued until later in the evening, with the main frontal precipitation band quickly followed by a more showery area of precipitation in northwesterly flow beginning around 1800 MST. Echo heights were somewhat lower, around 17,000 - 19,000 feet (5200 - 5850 m) during this second period of precipitation associated with the core of the trough, and reflectivity values decreased somewhat also (mostly 20-30 dbz). As icing activity increased overnight and into the morning hours of the 14th, available satellite images show warming tops once again. Radar images continue to suggest light snowfall through around 0800 MST on the 14th over the Brian Head area. This precipitation also appeared somewhat orographic in nature, and overnight VAD profiles showed varying heights to the echo tops, often exceeding 20,000 feet (6150 m). It appears that the light overnight precipitation (i.e. 0000 – 0800 MST on the 14th), which looks from the VAD profiles to have at least partially originated from a higher deck over 20,000 feet (6150 m), was not enough to prevent significant icing activity at the site. It appears also that there was orographically induced precipitation during this second icing period of icing, as suggested by higher local reflectivity values in the close vicinity of the Brian Head site (to 25+ dbz), with most of the surrounding reflectivity values under 20 dbz. Morning visible satellite images on the 14th suggested a rather thick mid-level deck (high opacity) with some mountain-wave features indicating stability near the top of the deck. A fairly solid mid-level deck persisted through most of the day on March 14, but may have either changed in elevation or thinned enough to result in a sharp decrease in the icing activity.

Nearby SNOTEL sites indicated increases of 1.0 – 1.5 inches (2.5 – 5.0 cm) of snow water content from about midday on March 13 through the morning of the 14th. Precipitation measurements at the SNOTEL sites were somewhat less, about 0.5 – 1.2 in (1.3 – 3.0 cm) but may have suffered from some gage catch deficiency due to wind or other factors.

This case is a good illustration of changes in precipitation efficiency, with deep cloud development and associated precipitation resulting in high efficiency during the main precipitation periods, flanked by low-efficiency periods both pre-frontally and in the post-trough environment. Figure 17 is a chronological plot of the relative precipitation efficiency in 3-hour time blocks, obtained by comparing the precipitation and icing amounts in each time period. The presence of SLW, as evidenced by ice detector de-icing cycles, is considered to be indicative of untapped (seedable) SLW, thus less than optimal

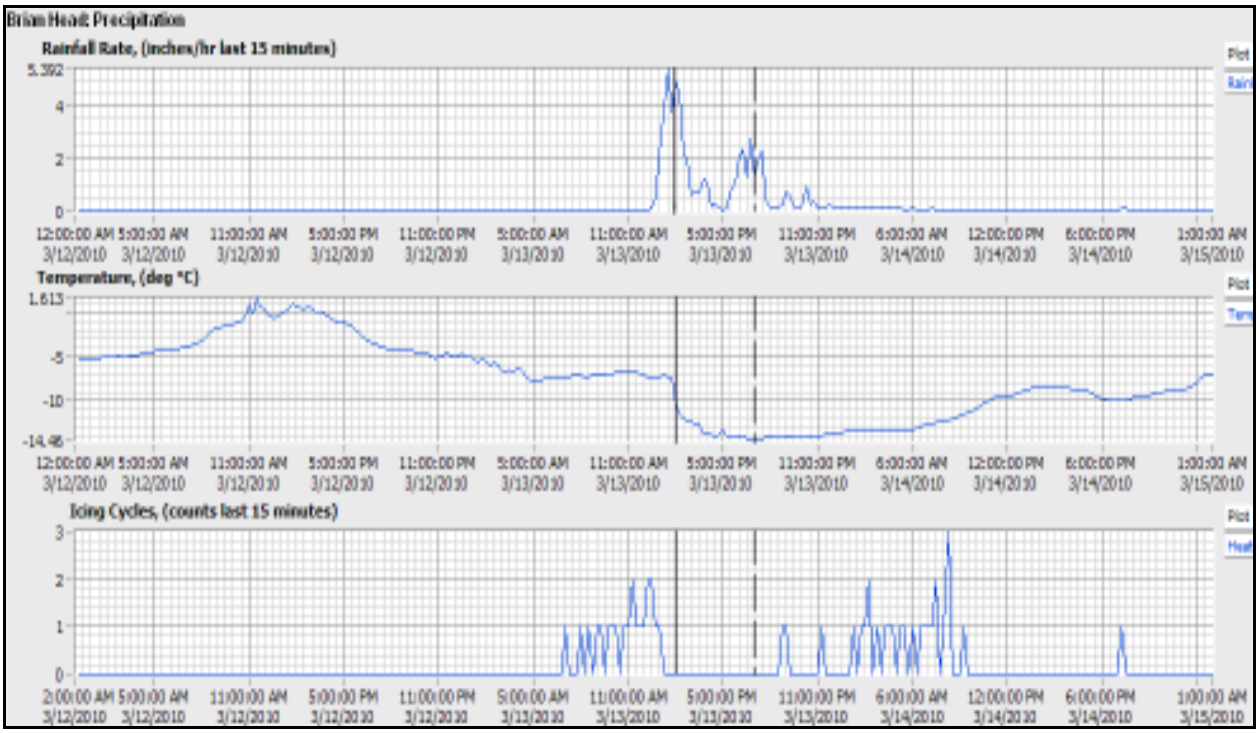

Figure 12. **Brian Head time series of precipitation, temperature, and icing for March 12-14, 2010. Approximate times of cold frontal passage (solid vertical line) and upper-level trough passage (dotted line) are shown.**

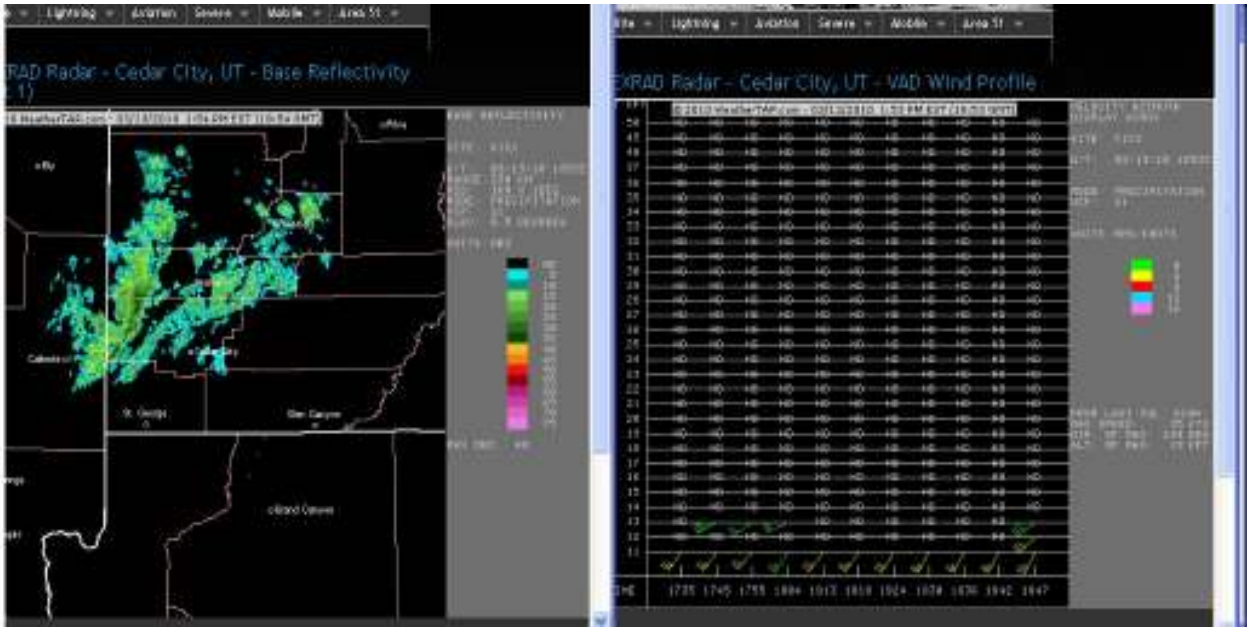

Figure 13. **Radar reflectivity and vertical time section of winds at 1154 MST on March 13, 2010, illustrating the low cloud tops (with precipitation echoes below about 12,000 feet) at the leading edge of the frontal precipitation band.**

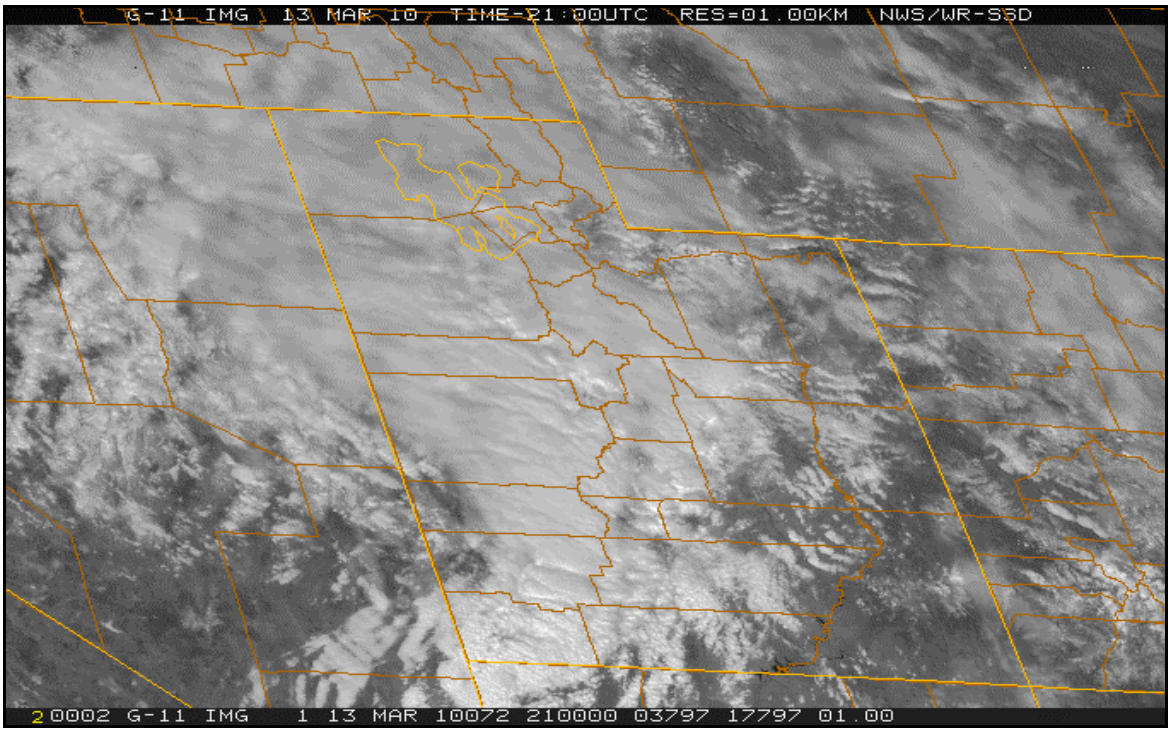

Figure 14. Visible spectrum satellite image at 1400 MST, March 13, 2010, as the frontal precipitation band moves across the area.

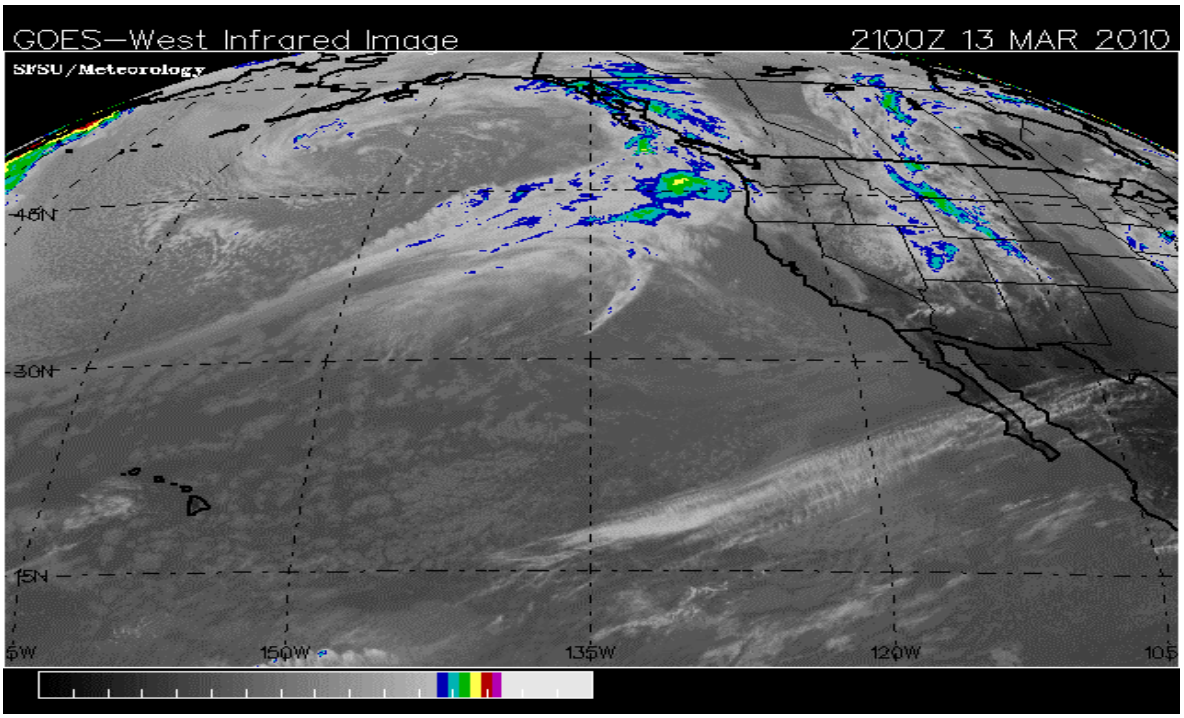

Figure 15. Infrared satellite image at 1400 MST, March 13, 2010, showing colder cloud tops associated with the main frontal band.

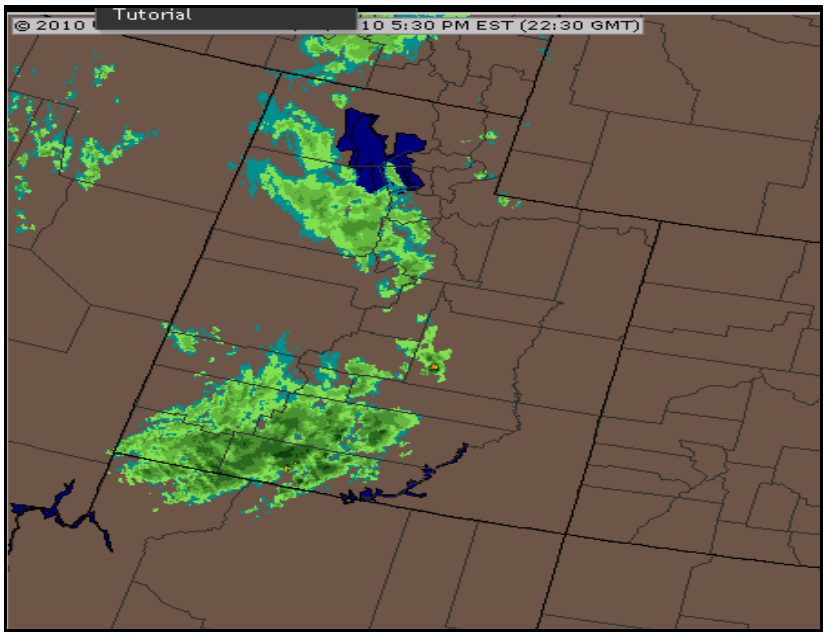

Figure 16. Radar Image at 1530 MST, March 13, 2010

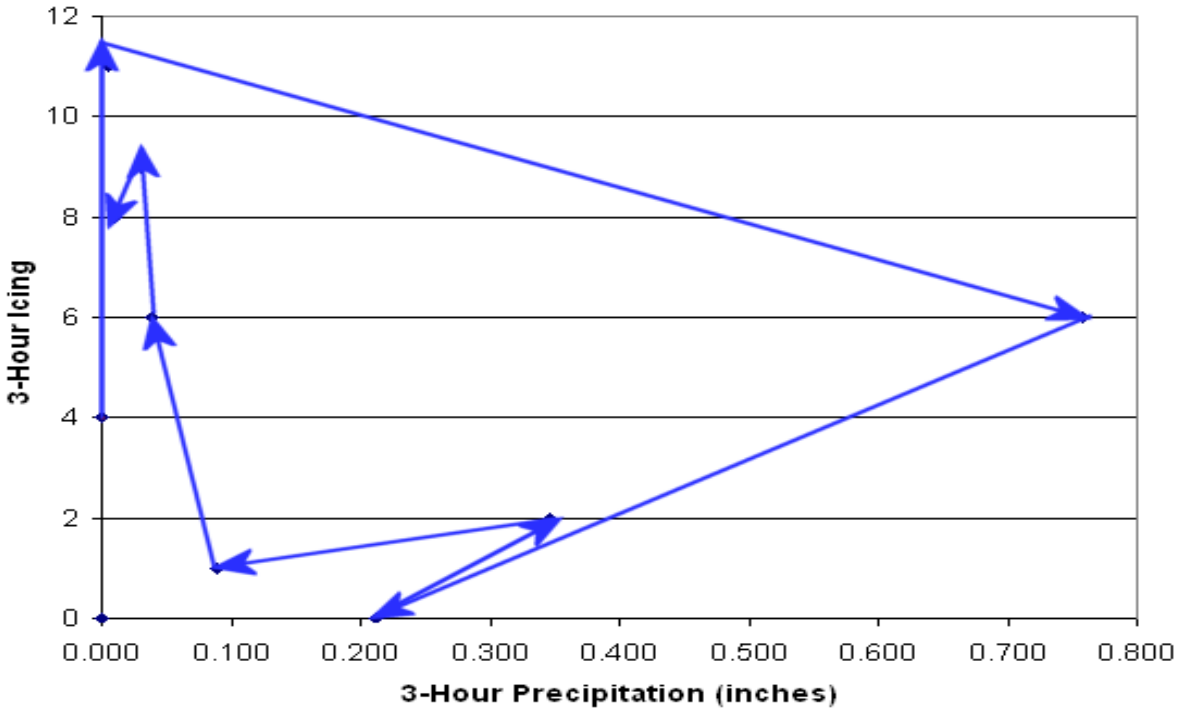

Figure 17. Relative precipitation efficiency in 3-hour blocks, the first ending at 0900 on March 13 and the final time block ending at 0900 on March 14, 2010.

precipitation efficiency. The term "relative" is used to highlight the relationship between icing and precipitation during a given period. High precipitation combined with low icing (lower right portion of the plot) would suggest relatively high efficiency. Conversely, a high amount of icing in conjunction with little or no precipitation (upper left portion) would suggest relatively low efficiency. Also, it is worth noting (refer to Figure 12) that all the icing observed in this case was either pre-frontal or post-trough, with no icing observed during the approximately 5-hour period between the cold front and the upper-level trough passage. This may be due to the presence of some drier air in this sector of the storm, or to other factors.

Stability analysis for the pre-frontal icing period on March 13 shows that the Cedar City airport varied from about 4° to 8°C with the Brian Head site near –7°C during this period. The dew point at Cedar City rose from about –2° to 0°C during this period, with the Cedar City observations implying a well-mixed atmosphere and a cloud base near to a little colder than freezing. The timing of the cold front was nearly identical for both Cedar City and the Brian Head site, between 1300 and 1400 MST on the 13th. The post-frontal icing period early on the 14th was associated with Brian Head site temperatures near –12° to –13°C, and a temperature of –2° to –3°C with near saturation at Cedar City. This indicated that the atmosphere remained well mixed on the 14th.

5. CONCLUSIONS

Some general conclusions are summarized below, based on analysis of the existing data, but these must be considered preliminary due to the limited nature of the data set. Future seasons of data collection will provide more confidence in the conclusions that are reached.

1) Although some meteorological patterns and relationships showed good correspondence with the occurrence of seedable conditions, providing reasonable prediction capability, it has become clear that **real-time** monitoring of the ice detector data is of significant value in seeding opportunity recognition.

2) The ice detector data suggest that in the vast majority (perhaps 80-90%) of icing periods in Utah, low-level atmospheric stability would not be sufficient to inhibit orographic lofting of ground generator seeding plumes into the SLW zones in winter clouds. Low-level stability is most common during the early- and mid-winter season (December – January).

3) Icing at a given location is sensitive to surrounding terrain, as well as site-specific wind conditions. Icing activity observed at a given mountain-top location tends to be heavily clustered into certain wind direction sectors, which vary widely depending on the site. The implications are that lifting of the low-level (valley) air mass over significant mountain barriers tends to be much more efficient in certain areas (such as canyons and terrain "catch" areas), while much of the low-level air mass will move around barriers when possible, especially if there is any thermodynamic stability.

4) During storm periods, icing intensity tends to be negatively correlated, in approximately a linear way, with precipitation intensity. This makes intuitive sense, since the amount of SLW at any given time and location is a function of the rate of production (due to lifting of a saturated air mass) minus the rate of decay (due to scavenging by precipitation, the nucleation process, and riming on solid surfaces). Intense icing activity is most often observed between significant precipitation periods during storm events.

5) The bulk of icing activity occurred when site temperatures ranged from approximately –6° to –12°C, although significant activity can occur outside that range.

6) Icing activity is positively correlated with wind speed, which is due to two primary factors: a) the rate of forced orographic lift over the local terrain, and b) flux past the icing sensor, both of which increase as wind speed increases.

7) Synoptically speaking, icing at these sites occurs most often after passage of the 500-mb trough axis. Icing during these periods accounts for nearly 50% of the total activity. Significant icing also occurs between the surface frontal passage and trough axis passage (approximately 25%), and to a lesser degree during pre-frontal or poorly defined situations. A special case of

"poorly-defined" situations includes closed-low type of systems which are relatively common in the southwestern U.S., but seem to account for well under 10% of icing activity. These observations suggest that seedability may be greatest in post-trough situations, in cases where cloud depth is sufficient to produce accumulating snowfall in the target areas. These situations also tend to be associated with a well-mixed lower atmosphere and colder mid-level temperatures in general, both of which are favorable conditions for cloud seeding. The data also suggest that icing is more common after the end of storm-related precipitation than before the onset of precipitation, although the majority of icing activity occurred either between or during precipitation periods within a storm event. In addition, it was found that any pre-precipitation icing typically begins within a few hours prior to the initial onset of precipitation, but that icing may continue for several or occasionally 12+ hours after storm precipitation ends.

8) Analysis of diurnal cycles in icing activity did not produce very clear overall results, but may still be worth investigating in future analyses. It may be that the diurnal cycle is very site-specific (as large site to site variations were found), or simply that more data is required to conduct a reasonable analysis. There are several factors (some entirely meteorological in nature, and others related to the instrument detection of SLW) that are believed to have an effect on the diurnal distribution of rime ice accumulation. Comparison of diurnal cycles in icing and in precipitation activity may also result in some important implications related to precipitation efficiency, as investigated in this season's data at Brian Head. More data is needed to make any firm conclusions regarding the diurnal behavior of icing activity.

9) Although there was no quantitative cloud-top temperature data in this study, basic qualitative analysis from IR satellite images shows a general relationship between warmer (lower) cloud tops and increased icing. This is noted in some of the case studies. Cloud top temperature is loosely related to precipitation intensity, with many instances of colder cloud tops corresponding to periods of heavier precipitation, much of which likely originates in these higher (colder) cloud decks. This dramatically increases the decay rate of SLW produced in lower decks or lower portions of the same cloud deck, due to scavenging by precipitation particles, and in turn may decrease the seeding potential when colder cloud tops are present.

6. ACKNOWLEDGEMENTS

The support and cooperation of the following agencies is gratefully acknowledged.

- Lower Basin States: funding for the ice detector equipment, its installation and post-season data analysis. The LBS contributors include:
  - The Six Agency Committee – California
  - Central Arizona Water Conservation District
  - Southern Nevada Water Authority

- Utah Division of Water Resources: administration of funds for the ice detection systems initiative and provision of high-resolution ETI precipitation gages.

- Utah Department of Transportation for site use and data link at Skyline

- Brian Head Ski Area for site use

- Emery County Water Conservancy District: use of data from an ice detector system located near Fairview, Utah.

- Sanpete County Water Conservancy District: use of data from an ice detector system located near Fairview, Utah.

7. REFERENCES

Solak et al., 1988: Ground-Based Supercooled Liquid Water Measurements in Winter Orographic Clouds. J. Wea. Modif., Vol. 20 No.1, pp. 9-18.

Solak et al., 2005: Observations of Rime Icing in the Wasatch Mountains of Utah: Implications for Winter Season Cloud Seeding. J. Wea. Modif., Vol. 37, pp. 28-34.